Superconducting Integrated Receiver development for TELIS

R.W.M. Hoogeveen[*1a], P.A. Yagoubov[a], A. de Lange[a], A.M. Selig[a],
V.P. Koshelets[b], B.N. Ellison[c] and M. Birk[d]
[a] SRON Netherlands Institute for Space Research, Utrecht, the Netherlands
[b] Institute of Radio Engineering and Electronics, Moscow, Russia
[c] Rutherford Appleton Laboratories, Chilton, Didcot, United Kingdom
[d] Deutsches Zentrum für Luft- und Raumfahrt, DLR-IMF, Oberpfaffenhofen, Germany

ABSTRACT

TELIS (TErahertz and submm LImb Sounder) is a cooperation between European institutes, DLR, RAL, and SRON, to build a three-channel balloon-borne heterodyne spectrometer for atmospheric research. Many atmospheric trace gases have their rotational transitions in the sub millimeter and THz range, yielding a very rich spectrum. Limb sounding results in very accurate vertical profiles.

All three TELIS receivers will operate simultaneously. The 500 GHz channel is developed by RAL and will produce vertical profiles of BrO, ClO, O_3, and N_2O. The 1.8 THz channel is developed by DLR and will mainly target the OH radical, and will also measure HO_2, HCl, NO, NO_2, O_3, H_2O, O_2, and HOCl. Finally the 550 - 650 GHz channel is developed by SRON and IREE and will measure profiles of ClO, BrO, O_3, HCl, HOCl, H_2O, and its 3 isotopologues, HO_2, NO, N_2O, HNO_3, CH_3Cl, and HCN.

TELIS will fly on the MIPAS-B2 gondola. The two instruments together will yield the most complete set of stratospheric constituents. The qualification flight is foreseen in the winter of 2006/2007.

The TELIS instrument serves as a test bed for many novel cryogenic heterodyne technology: novel low-noise cryogenic heterodyne mixer detectors, novel low-noise cryogenic intermediate-frequency amplifiers, novel back-end spectrometer. In the presentation these technologies will be discussed and compared with 'standard' technology as applied in the Microwave Limb Sounder (MLS) on EOS-Aura, launched in 2004. Emphasis will be on the science and technology of the channel developed by SRON. It contains a Superconducting Integrated Receiver (SIR), which combines on a 4x4 mm^2 chip the low-noise Superconductor-isolator-Superconductor (SIS) mixer and its quasi-optical antenna, a superconducting phase-locked Flux Flow Oscillator (FFO) acting as Local Oscillator (LO) and SIS Harmonic Mixer (HM) for FFO phase locking. Latest test results and retrieval simulations will be presented.

Key words: Atmospheric, limb-sounding, cryogenic, heterodyne, sub millimeter.

1. INTRODUCTION

For the study of the Earth atmosphere there are several observational strategies. Most obvious is to perform measurements in the UV/visible region of the spectrum, where reflected sun light carries the spectral absorptions of trace gases. Band pass filters and/or gratings provide spectral discrimination. Examples are the SBUV and TOMS instruments on the NIMBUS-7 and several subsequent satellites [1], and more recently full spectrometers such as ERS-2/GOME [2], ENVISAT/Sciamachy [3], EOS-Aura/OMI [4], and MetOp/GOME-2 [5]. Another possibility is to measure the emission of the atmosphere in the thermal infrared part of the spectrum, as is employed by ENVISAT/MIPAS [6], Aura/TES [7], MetOp/IASI [8] and many other instruments. Here a Michelson interferometer provides the spectral discrimination.

A third possibility is to employ the millimeter and sub-millimeter frequency range where simple light weight molecules have their rotational transition lines. Using standard optical spectroscopic methods is not possible for high resolution spectroscopy as it would require huge gratings or very cumbersome mechanics for a Michelson-type

[1] * SRON, Sorbonnelaan 2, 3584 CA, Utrecht, the Netherlands. R.Hoogeveen@sron.nl, phone +31 30 253 5703, fax +31 30 254 0860, www.sron.nl.

spectrometer. For the millimeter and sub millimeter wavelength region heterodyne detection is well known and very high resolution (in excess of 10^6) can be obtained. The principle of heterodyne detection is to add to the incoming atmospheric radiation a strong Local-Oscillator (LO) signal a few GHz away from the frequency band of interest. The combined atmospheric and LO signal is detected by a so-called mixer detector. This is a non-linear detector that in principle should output signals at the original frequencies, at the sum frequency (and higher harmonics) and at the difference frequency. Due to speed limitations in the mixer, in practice only the difference frequency will be detectable. The amplitude of this so-called Intermediate Frequency (IF) is proportional to the strength of both the LO signal and the atmospheric signal, and can thus be boosted by using a strong LO signal. The IF signal is amplified and standard radio techniques are employed to create a spectrum which contains all the information of the incoming atmospheric signal.

Application of the heterodyne detection technique in atmospheric observations has been pioneered by the Microwave Limb Sounder on board the UARS satellite [9], launched in 1991. UARS/MLS measured stratospheric ozone, ClO, water vapor, pressure, and temperature using bands at 63, 183, and 205 GHz. UARS/MLS has operated up to 1999.

Its improved successor MLS on board of EOS-Aura has been launched July 2004 [9]. The frequency bands have been extended to 118 GHz (for temperature and pressure), 190 GHz (H_2O and HNO_3), 240 GHz (O_3 and CO), 640 GHz (for HCl, ClO, BrO, HO_2, and N2O), and 2.5THz (for OH). The EOS/MLS instrument performs very successfully.

In Europe, the Swedish ODIN satellite [10] carries the Sub Millimeter Radiometer instrument which is used for atmospheric research as well as for astronomical observations. Its frequency bands are located at 118.25 - 119.25 GHz, 486.1 - 503.9 GHz, and 541.0 – 580.4 GHz. ODIN was launched in 2002 and is still operational.

The key element of a heterodyne receiver is the mixer. Traditionally, the mixer consists of Schottky diodes. These can be operated either uncooled (MLS) or cooled (100 K for ODIN/SMR). Cooling significantly reduces the noise temperature of the mixer. A major drawback of Schottky mixers is the LO power needed. Especially at the higher frequencies the LO-power requirement excludes the use of solid-state devices and necessitates cumbersome gas lasers: Aura/MLS carries a CO_2-laser pumped methanol laser to generate the required LO power at 2.5 THz.

A huge performance improvement is gained by employing superconducting mixers at cryogenic temperatures (4 K) such as Superconductor-Insulator-Superconductor (SIS) mixers or Hot-Electron Bolometer mixers (HEBM). In fact, two satellite instruments are currently under development using such mixers: JEM/SMILES [11] and Herschel/HIFI [12]. The Japanese SMILES instrument (Superconducting Sub millimeter-Wave Limb Emission Sounder) for the Japanese Experiment Module (JEM) of the International Space Station will observe atmospheric species at 625 and 650 GHz. Launch has been delayed to 2008. The first to use cryogenic mixers will be the HIFI instrument (Heterodyne Instrument for the Far Infrared) on board the astrophysical Herschel satellite. This instrument is currently under assembly and test at the SRON laboratories and will be launched in 2007.

Recently JPL proposed a cryogenic successor for their MLS series [9]. The Scanning Microwave Limb Sounder (SMLS) contains a mm (180-280 GHz) and two submm (580 – 680 GHz) SIS-based receiver channels.

Extrapolating the current trends towards the future we foresee Earth limb sounding from a satellite platform with superconducting receivers operating at millimeter, sub millimeter and Terahertz frequencies. Instead of gas lasers only solid-state local oscillators are to be employed to reduce system complexity. To fully exploit the sensitivity gain by the cryogenic mixers, also low-noise IF-amplifiers are needed. Here the trend is to employ the GaAs and InP High Electron Mobility Transistor (HEMT) amplifiers. As back-end spectrometers the most likely candidates are Acousto-Optic Spectrometers or Digital Auto Correlators, in contrast to the current low-resolution filter-bank spectrometers.

Several balloon and aircraft instruments anticipate space application of new cryogenic technologies, as well as ground based astronomical observatories. Without being complete a few examples are given. Already operationally flying instruments for Earth observation using SIS mixers are: PIROG [13], ASUR [14] and BSMILES [15].

Recently three European institutes (DLR, SRON and RAL) have decided to develop a high sensitivity, balloon-borne atmospheric sounder that will allow simultaneous measurement of many key stratospheric constituents. The instrument is called TELIS (TErahertz and submm LImb Sounder) and will provide vertical profiles of a.o. OH, HO2, O3, N2O, CO, HCl, HOCl, ClO, and BrO that are associated with the depletion of stratospheric ozone and climate change. The ambitious science goals of the TELIS instrument is accomplished by use of three independent frequency channels: 500 GHz, 550 - 650 GHz and 1.8 THz. All channels will use a state-of-the-art superconducting SIS and HEBM technology. In addition, TELIS will serve as a test bed for a number of novel technologies in the field of low-noise cryogenic heterodyne detection, such as the low-noise cryogenic IF amplifiers and digital auto-correlator spectrometers.

TELIS will fly on the MIPAS-B balloon platform. MIPAS-B is a Fourier Transform Spectrometer developed and operated by the Institute of Meteorology and Climate research of the University of Karlsruhe, Germany [16], and will simultaneously measure in the range 680 to 2400 cm^{-1}. The combination of the TELIS and MIPAS instruments will provide a wealth of scientific data, both as a stand alone chemistry mission and in complement to existing space borne instruments, e.g., ENVISAT, Aura and METOP.

The first (qualification) flight of the TELIS instrument is foreseen in the winter of 2006/2007.

In the next sections, first the science and general design of the TELIS instrument will be discussed. Next the details of the SIR channel will be given, as well as the retrieval simulations and sensitivity studies. Actual status will be given in the last section.

2. THE SCIENCE OF TELIS

The TELIS receivers combine a high frequency resolution and low noise observations with limb sounding, enabling the determination of vertical profiles of very weak individual lines. This results in an extensive list of molecular species that can be targeted: BrO, ClO, HCl, HOCl, CH_3Cl, O_3 (normal and isotopic), H_2O (normal and isotopic), OH, HO_2, HNO_3, NO, N_2O, NO_2, HCN, CO, and O_2.

With respect to stratospheric ozone depletion the halogen, NO_x and HO_x chemistry can thoroughly be investigated. Isotopic water may shed light on the origin of stratospheric water while ozone isotopes may give insight in hidden and unknown chemical reactions.

A key question in stratospheric sciences is whether ozone will recover in the coming decades as a result of international regulations on ozone depleting substances. In the lower and middle stratosphere ozone depletion is fairly well understood. The fact that TELIS can retrieve almost all species appearing in the catalytic ozone depletion cycles will put the existing atmospheric chemistry models to stringent tests. In the upper stratosphere chemistry models are less accurate: ozone concentrations are underpredicted, HO_2 is underpredicted, and OH is overpredicted [17,18]. Observing all species simultaneously will shed light on the production and loss mechanisms of HO_x and the partitioning between OH and HO_2.

Stratospheric water vapor plays an important role in the ozone chemistry as a source gas for the production of HO_x. In addition, in polar regions Polar Stratospheric Clouds (PSCs) are formed during the winter and inactive bromine and chlorine species are transformed by heterogeneous reactions on the PSCs, into active bromine and chlorine. In the local spring, the PSCs evaporate and the reactive Br/Cl radicals are released giving rise to the well known ozone holes.

The origin is of stratospheric water is still not completely understood. Stratospheric water is formed in situ by the oxidation of species, for instance, methane, and is transported from the troposphere through the limiting cold trap of the tropopause. The accurate measurement of water isotopologues may give insight in the relative weights of the water loading mechanisms of the stratospheric, as the different masses and energy level structures of the isotopologues result in different rates in evaporation, condensation, and chemical reactions.

Statistically it is expected that $^{49}O_3$ and $^{50}O_3$ have relative abundances of respectively 1.10‰ and 6.09‰. Space-borne and ground measurements of stratospheric $^{50}O_3$ shows typical enrichments of 10-20% [19]. Laboratory experiments have shown that the reaction rate of $O + O_2$ is strongly dependent on the isotopes involved: for instance, $^{16}O + {}^{18}O^{18}O$ is the fastest reaction and is 50% faster than $^{16}O + {}^{16}O^{16}O$ [20]. This difference in the formation rates, however, is not sufficient to explain the observed deviation from statistical abundances. Measuring the 'normal' ozone along with the most abundant isotopic compounds may give insight in the mechanism behind this anomaly, and may reveal others.

3. TELIS INSTRUMENT DESCRIPTION

The optical front-end of TELIS is common for the three channels and consists of a pointing telescope, calibration blackbody, and relay and band-separating optics, see Figure 1 and [21, 22, 23]. The telescope is a dual offset Cassegrain antenna. Primary, secondary, and tertiary mirrors of the telescope are mounted on a common frame. The complete unit is rotated around the axis coinciding with the direction of the output beam. Primary parabola has an elliptical cross-section of 260x140 mm. A 2:1 anamorphicity is introduced by the cylindrical tertiary mirror to improve telescope mass, compactness, and moment of inertia. A vertical (elevation) resolution at the tangent point is about 2 km at 500 GHz (FWHM), inversely proportional to the frequency. Horizontal (azimuth) resolution is about a factor of 2 worse.

Radiometric calibration is performed using two blackbody reference sources: in every antenna scan the hot-load and the cold sky is observed. , The cold sky reference is measured with the telescope set at 40 degree upwards with respect to the limb position. The hot load consists of a conical black-body at the ambient temperature, and can be observed by switching a mirror between the telescope and the warm optics.

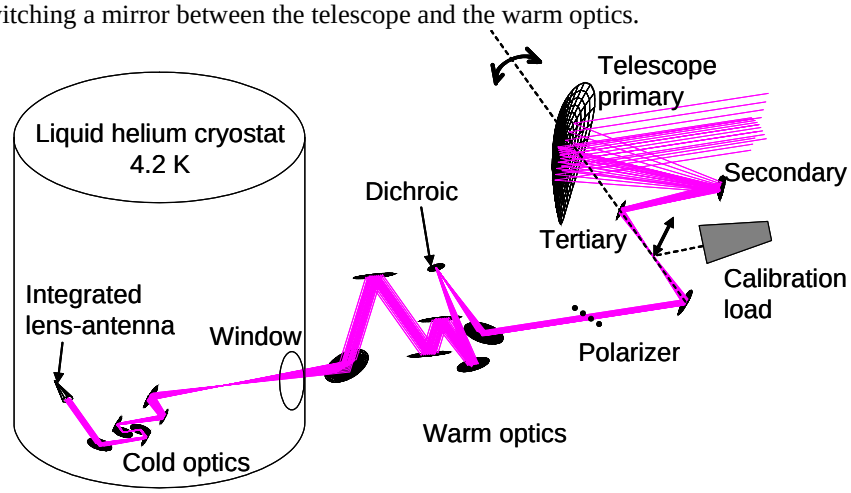

Figure 1. Schematics of the TELIS front-end optics and the SIR channel optics. The telescope unit is rotated around the axis coinciding with the direction of the output beam. A wire grid polarizer and a di-chroic plate are used to separate the beam into the three frequencies of the three channels (only 550-650 GHz channel is shown). The cold optics and mixer elements of the three channels are located inside the cryostat at the ambient temperature of 4.2 K.

Frequency separation between the channels is performed quasi-optically. First, a wire grid reflects one linear polarization component into the 500 GHz channel. The transmitted component is split by a di-chroic filter, and off-set reflectors are used to interface the optics from the telescope to the cryogenic channels. The three beams then enter a custom designed liquid-helium cooled cryostat through three optimized windows. Figure 1 shows schematics of the optics directly related to the 550-650 GHz channel. The optical beams and the mirrors of the two other frequency channels are not shown.

Inside the cryostat the receivers have dedicated cold optics, mixing element and IF amplifiers.

The 500 GHz receiver channel is being developed by RAL and is based on a highly successful airborne instrument [24] and similar to band E of the MASTER instrument proposed for the ACECHEM mission [25]. It is a highly compact unit consisting of a fixed-tuned waveguide SIS mixer, cryogenic solid-state local oscillator (LO) chain and a low-noise Intermediate-Frequency (IF) chain. Single sideband[2] operation is achieved through use of a miniature cryogenic di-chroic filter that provides a 4 K image termination and image band rejection of >25dB. For optimization of the di-chroic single sideband filter a high IF is chosen: 14 – 18 GHz.

The 550-650 GHz receiver channel is being developed in cooperation between IREE and SRON and is based on a single-chip Superconducting Integrated Receiver (SIR) that comprises on one 4 x 4 mm^2 substrate a low-noise SIS mixer with quasi-optical antenna and a superconducting Flux Flow Oscillator (FFO) acting as LO [26]. Tunability of the FFO shall allow for a wideband operation of this channel, with a goal to obtain 100 GHz instantaneous rf bandwidth or even more. The SIR channel is discussed in detail in the next section.

The 1.8 THz channel is being developed by DLR, also acting as Principle Investigator (PI) for the TELIS mission. It is based on a phonon-cooled NbN HEBM technology, similar to that under development for SOFIA by MSPU and DLR **XX TBC** [27]. It utilizes a cryogenic solid-state LO coupled to the mixer via an optical interferometer (Martin Puplett type). Single sideband[2] operation is obtained by another Martin Puplett interferometer. The channel is designed to allow future upgrade to 2.5 or 3.5 THz, where more favorable emission lines of the OH radical can be observed.

Three amplified output IF signals are fed to an IF processor which converts the IF to the input frequency range of the digital autocorrelator of two times 2 GHz bandwidth. Both IF processor and digital autocorrelator are developed by the Swedish Omnisys company [28].

An on-board PC-104 computer interfaces with the control electronics of the three receiver channels and the instrument, with the digital auto correlator, with the host instrument MIPAS, and with the ground segment through a

[2] In heterodyne detection the difference signal between the Local Oscillator and the atmospheric signal is amplified. As this difference can be positive and negative, two frequency bands above and below the LO are detected simultaneously. Single-sideband filters transmit the signal band of the atmospheric signal and block the image sideband.

radio link. The ground segment consists of a server computer interfacing with three dedicated client computers through TCP/IP socket connections.

4. OPTICS OF THE SIR CHANNEL

The layout of the 550 - 650 GHz SIR channel cold optics is shown in Figure 2 and discussed in more detail in [21-23]. The input beam of the SIR channel cold optics is a "parallel" and frequency independent beam with a waist radius of 11.0 mm. The off-axis parabolic mirror (L1) focuses the beam to minimize the sizes of the cryostat window (L2) and the infrared absorption filter (not shown in the Figure 2).

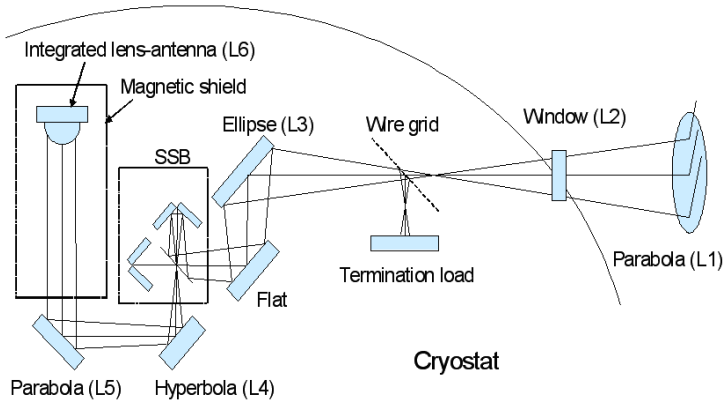

Figure 2. Layout of the cold channel optics. Lines show the optical beam trajectories.

A polarizing wire grid provides the injection of a cold load for the image band. The ellipse L3 serves as an optical relay and minimizes the beam size inside the Martin-Puplett single sideband[2] (SSB) filter. The hyperbola L4 and parabola L5 image the system-pupil on the Silicon elliptical lens (L6), and on the integrated antenna of the chip, located at the back surface of L6. The SIR channel cold optics is frequency independent allowing for wide-band operation.

All optical components have a minimum diameter of 4 beam radii (1/e field level), corresponding to an edge taper of -35 dB. Only the integrated lens is smaller than 4 beam radii.

The quasi-optical performance of the SIR cold optics as well as the complete TELIS instrument has been verified using the GRASP8 package [29]. The sensitivity of the integrated lens-antenna system has been calculated by PILRAP (Program for Integrated Lens and Reflector Antenna Parameters [30]). Figure 3a shows the calculated 2-D far field pattern of the receiver at 625 GHz. The pattern exhibits the expected elliptical form, as determined by the anamorphicity of the telescope (note different scale in azimuth and elevation). The asymmetry in the azimuth plane, caused by the fast off-axis optics of the telescope, is unimportant as the atmosphere is assumed to be horizontally uniform. Figure 3b shows the vertical cut of the antenna pattern at azimuth 0 degrees and the Azimuthally Collapsed Antenna Pattern (ACAP). The ACAP is symmetric and has an almost Gaussian shape for amplitudes larger than -20 dB. An asymmetric side lobe starts at the -25 dB level. The FWHM of the ACAP at 625 GHz is 0.17 deg, corresponding to a 1.65 km FWHM beam at the tangent point in 550 km distance. This beam shape will be relevant for the retrieval of atmospheric data and has to be considered in the retrieval model.

An extensive alignment and tolerance analysis has been performed, using the program ZEMAX for geometrical optics analysis and GRASP for physical optics analysis. Details can be found in ref. [21,22]. The optical configuration of the TELIS SIR channel was considered as three sub-assemblies: telescope, warm optics, and cold channel. In the analysis it was assumed that the optical shape of the mirrors is perfect, and that only the position and alignment is off. In [23] the effects or surface irregularities are studied.

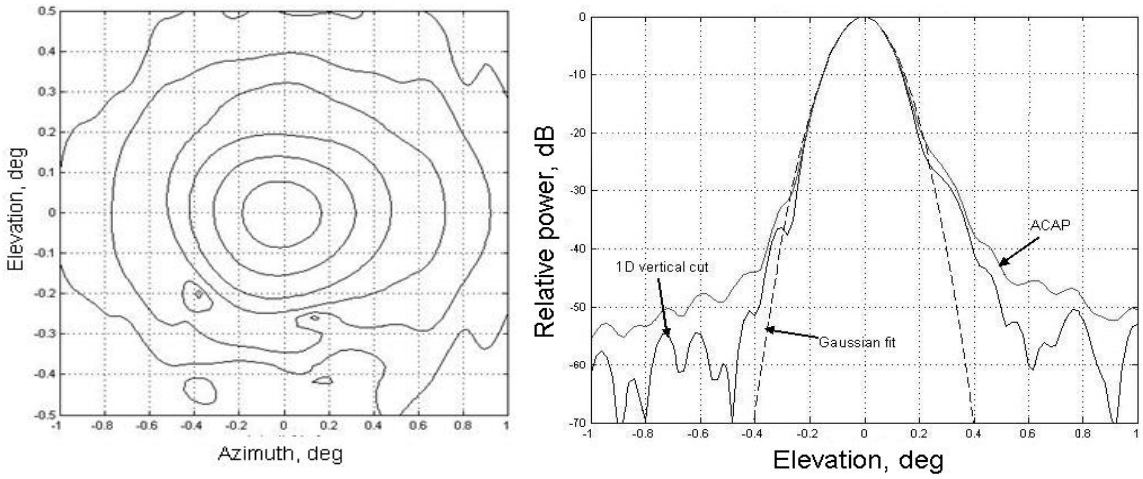

Figure 3a, left: The far field 2-D antenna pattern of the complete SIR channel at 625 GHz. Solid lines represent the -3 dB and the -10 dB to -50 dB contours. Figure 3b, right: Vertical cut of the antenna pattern at azimuth 0 degrees and the Azimuthally Collapsed Antenna Pattern (ACAP). A Gaussian fit is given as a reference.

The main conclusions from the alignment and tolerance analysis are:

- Typical angular tolerance within the cold optics is 0.06-0.08 degrees corresponding to a linear tolerance of about 20 micrometers.
- Within the warm optics, the typical angular tolerances are 0.1-0.2 deg, translated to about 30 micrometers requirements for the production.
- The telescope to warm optics tolerance is ±1 mm for lateral displacements and ±0.5 deg for misalignment.
- The warm optics to cold channel tolerance is ±1 mm for lateral displacements and ±0.3 deg for misalignment.
- The telescope should be aligned with visible light.

The tolerances on position and rotation of groups of elements can not be met. Therefore, two first (after the telescope) and last mirrors in the warm optics should have alignment possibility to (co)align the warm optics with the telescope and cold channel, respectively.

The components of the SIR cold optics are mounted on the common base plate using dead-reckoning. Alignment verification is performed using visible light to check for fabrication errors. Therefore, all reflective optical elements, including the telescope, have been fabricated with an optical surface quality.

5. THE SUPERCONDUCTING INTEGRATED RECEIVER

The most challenging part of the SIR channel is by far the phase-locked Superconducting Integrated Receiver (SIR) chip [26]. SIR comprises on one 4 x 4 x 0.5 mm^3 chip a low-noise SIS mixer with quasi-optical antenna, Flux Flow Oscillator (FFO) acting as Local Oscillator (LO) and SIS Harmonic Mixer (HM) for FFO phase locking, see Figure 4.

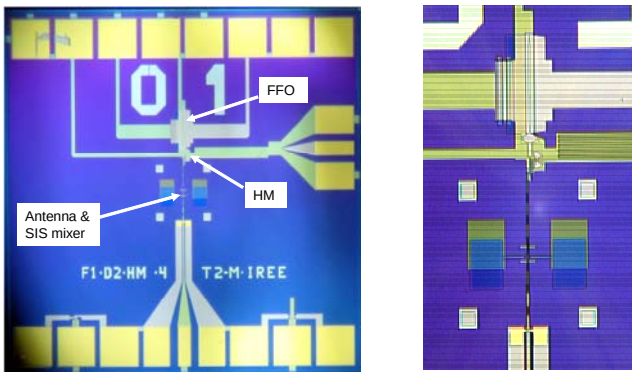

Figure 4. Microscope picture of the 4 x 4 mm^2 SIR chip (left side) and a zoom of the centre part (right side) consisting of an antenna-coupled SIS mixer, FFO as on-chip LO and HM for FFO phase locking. FFO, SIS, and HM are connected with microstrip transmission lines, which contain a number of RF-coupling and dc-blocking elements. The SIS mixer and FFO are provided with local magnetic fields via integrated control lines.

The FFO is a long Josephson tunnel junction in which an applied dc magnetic field and a bias current drive a unidirectional flow of fluxons, each containing one magnetic flux quantum. The velocity and density of the fluxons and thus the frequency and power of the emitted mm-wave signal may be adjusted independently by joint action of bias current and magnetic field. All components of the SIR microcircuits are fabricated in a high quality Nb-AlOx-Nb tri-layer on a Si substrate. The receiver chip is placed on the flat back surface of the Silicon lens, forming an integrated lens-antenna. To protect the FFO from external electromagnetic interferences the SIR chip is placed inside a cryo-perm inner shield and a superconducting lead-coated copper outer shield. The SIR chip is positioned away from the opening of the shielding cans, which is the only aperture for entering the signal beam and all electrical connections. This design leads to the higher f-number optics of the integrated lens-antenna configuration.

The spectral resolution of the TELIS spectrometer is 2 MHz. The FFO lineshape and stability should ideally be much better than this. As the free-running linewidth of the FFO can up to 10 MHz, the FFO is locked to an external reference oscillator using a Phase Lock Loop (PLL) system. For this, a small fraction of the FFO power is directed to a so-called Harmonic Mixer (HM). The HM is pumped by a tunable reference frequency in the range of 19-21 GHz from the Local oscillator Source Unit (LSU), phase locked to the internal ultra stable10 MHz Master Oscillator. The HM mixes the FFO signal with the n-th harmonic of the 19-21 GHz reference. The frequency of the LSU is chosen such that the difference frequency signal is about 4 GHz. This signal is amplified, down converted to 400 MHz, and compared with a 400 MHz reference. The phase-difference signal of the PLL is fed to the FFO control line current. Wideband operation of the PLL (15 MHz full width) is obtained by minimizing the cable loop length. The effect of the PLL on the FFO spectrum is shown in Figure 5. More on the PLL system can be found in [31]. Impact of the FFO spectrum on the retrieval accuracy is discussed in section 5.

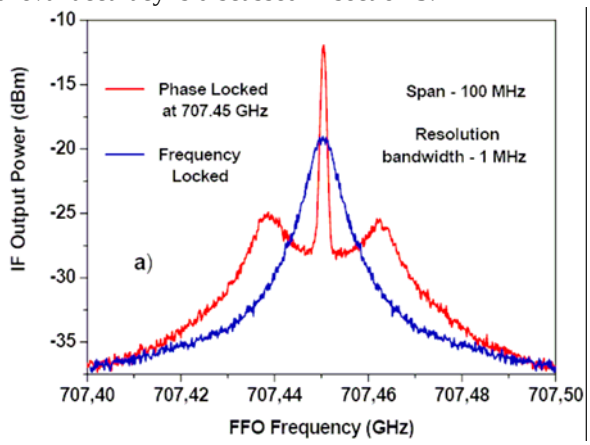

Figure 5: Spectrum of a frequency-locked FFO (blue curve) and phase-locked FFO (red). Due to limitations of the spectrum analyzer the central delta-peak of the PL-FFO appears broadened.

The IF signal of the SIR is amplified in two steps: about 32 dB gain is obtained by a 4-8 GHz cryogenic HEMT Low Noise Amplifier (LNA) based on InP transistors. The amplifier is integrated with Pamtech isolator. Figure 6 shows a picture of the amplifier/isolator and its measured gain and noise temperature at 4.2 K. Another 67 dB gain is obtained by an uncooled amplifier, outside the cryostat.

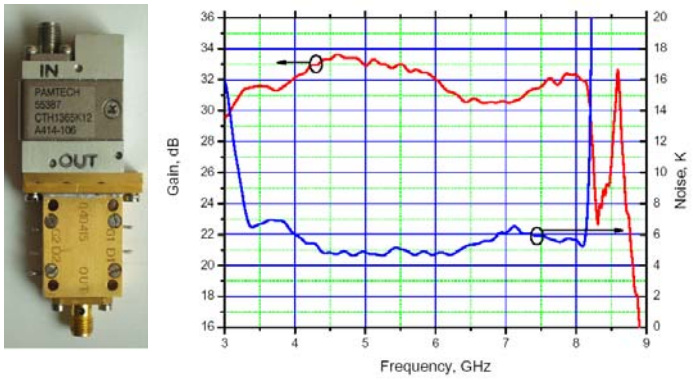

Figure 6: Picture of the integrated low-noise cryogenic intermediate frequency amplifier and isolator (left) and a plot of the measured gain and noise temperature.

In operation, the FFO can be regarded as a voltage-controlled oscillator of 484 GHz/mV. This requires very stable bias electronics. In the board design all precautions have been taken to reduce electromagnetic interference. E.g., a strict separation has been implemented between digital and analog signals, which also holds for the battery-based power supplies. Filter connectors and filter feed-through boards reduce pickup in the two meter cables between the electronics unit and the cryostat. The SIR device and its shields, the cold optics and all cold electronics are placed on a base plate. Heat straps connect the base plate to the cryostat bottom at places where heat is generated. Dedicated heat straps directly couple the SIR device to the cryostat bottom. The base plate is completely covered by thin aluminum plating to create a Faraday cage. Gaskets are applied to securely close possible chinks. However, measurements have confirmed that the largest leak for 5-7 GHz radiation is the entrance window for the atmospheric radiation. If needed a grid can be placed to block this radiation at the cost of some reduction of the atmospheric signal.

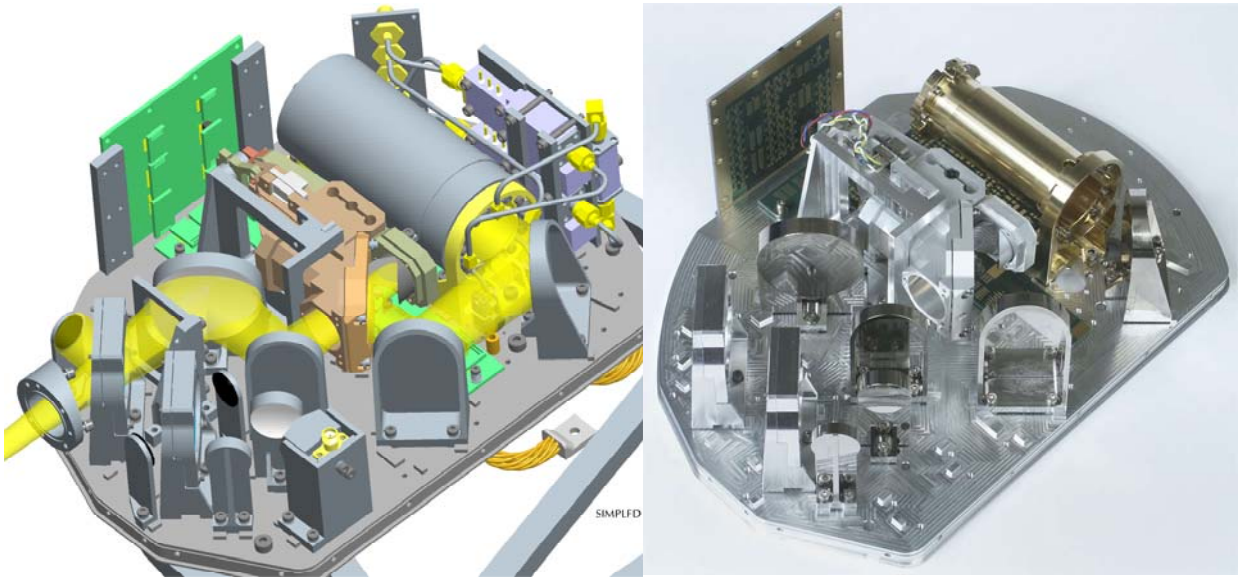

Figure 7: Design drawing of the TELIS-SIR cold plate and actual picture of it during the assembly procedure.

Figure 7 shows the design of the TELIS cold box (without the lid), and a picture of it during its assembly stage. The components encountered along the light path: cold-box entrance window and IR filter, polarizing grid for image-band separation and termination, alignment tool, ellipsoid mirror L3, flat folding mirror, Martin-Puplett interferometer acting as single-sideband filter, hyperbolic mirror L4, parabolic mirror L5, superconducting and anti-magnetic shields containing the SIR chip. Semi-rigid coax cables carry the 19-21 GHz reference signal to the SIR chip and IF signals from the chip to the IF amplifiers and isolator. Also visible are the green filter boards and some of the thermal straps.

6. RETRIEVAL SIMULATIONS AND SENSITIVITY STUDIES

Well before TELIS flights, the retrieval algorithms are set up to guide the instrument development and to determine instrument-sensitivity assessments. The retrieval is based on an iterative comparison between a calculated spectrum and the measured spectrum.

The calculated spectrum is determined by a so-called forward model. It calculates from the observation geometry the Line of Sight (LoS) and the Field of View (FoV). The emission spectrum is calculated by integrating the radiative transfer equation along the LoS, for a given temperature and pressure profile, and for assumed molecular density height profiles. The instrument model integrates over the FoV and adds instrument features such as noise and the instrument line shape, to determine the calculated TELIS spectrum. In the so-called inverse model, the calculated spectrum will be compared to the actual measured spectrum. Molecular density profiles will be altered iteratively to obtain the best match between modeled and observed spectrum. All limb scans are evaluated simultaneously to enhance the accuracy for the height profile.

The spectra in the forward model are based on the HITRAN database, 2004 edition [32]. Temperature and pressure profiles are taken from the standard US atmosphere in the simulations, while actual data will be used in the data retrieval. Scattering, and therefore sunlight, is negligible and therefore ignored. The frequency resolution is set to 2 MHz; the resolution of the spectrometer. The step height is 1 km and therefore half the estimated retrieval accuracy.

The instrument model includes all features that may alter the emission spectrum, such as instrument noise, calibration and its errors, baseline offset and drift, LoS/FoV and its errors, spectral line shape of the LO, standing waves, etc. Instrument noise and the LO lineshape are implemented in the instrument model, other features are in progress. In the retrieval simulations the impact certain instrument features will be assessed, and instrument or calibration requirements will be derived. It will also be investigated which features can be included as fitting parameters.

At present, two different inverse models are implemented; optimal estimation method (OEM) and Phillips-Tikhonov regularization. The main difference between the methods shows when the inversion problem is ill-posed which means that the measurement is insensitive to some parameters and not all desired information can be retrieved from the measured spectra. In the case of OEM, those parameters will be determined by the *a priori* information. The retrieved result, as well as its error, depends on the choice of *a priori* knowledge and its estimated accuracy. In contrast, the regularization method exploits only the measurement in this case and information may be added after the retrieval. Now, the optimum achievable information is retrieved, but it may be with low accuracy if the measurement is insensitive. If preferred, *a priori* information may be added, possibly introducing biased results.

Using the models described above, sensitivity studies are performed. Synthetic spectra are generated by the forward model assuming a model atmosphere and by adding the expected system noise. In the subsequent retrieval the difference between the retrieval results and the model atmosphere indicates the reference sensitivity of the system. If slightly different parameters are assumed in the retrieval than used in the forward model, deviations in the retrieved atmosphere with respect to the model atmosphere are indicators for the sensitivity of the instrument to these parameters.

As an example, the impact of the non-ideal spectrum of the SIR-FFO Local Oscillator has been studied using the HCl and ClO transitions at 625 and 650 GHz. As discussed in section 5, the free running FFO has a Lorentzian spectrum with a FWHM linewidth of 2 – 10 MHz. By the application of a phase-locked loop (PLL), the spectrum is sharpened into a delta peak. However, as not all power can be controlled by the PLL, two spectral side lobes appear that can contain a significant fraction of the FFO power (see Figure 5). Simulations have been performed with spectra of various line widths of the free running FFO, and with various fractions of phase-locked FFO power. In the retrieval models the impact of this non-ideal spectrum has been studied as well as the impact of an error in the knowledge of the spectrum.

The result of this study indicates that a non-ideal FFO spectrum smears the high-frequency structures of the spectrum [26], as expected. Due to the measurement noise, an error-free de-convolution is not possible. However, the retrieval of the HCl or ClO profiles are rather insensitive to the exact shape and knowledge of the FFO spectrum due to two facts: First reason is the atmospheric spectrum. For most observations the pressure broadening of the emission lines is much larger than the FFO linewidth while for the high-altitude measurement the separation between the narrow lines under study with the neighboring lines of other gases is much larger than the FFO linewidth. This implies that the convolution of the atmospheric spectrum with the FFO spectrum does not significantly degrade the possibility to determine the integrated line intensity. The second reason is the limb-observation strategy. Most information on the vertical profile is contained in the limb scans, and not so much in the spectrum itself. This is different from instruments with only one line of sight such as ASUR [14], where vertical information is solely retrieved from the spectral shape of the line.

This study will be extended to include all details of FFO frequency and phase locking.

7. ACTUAL STATUS

The TELIS-SIR channel is currently in the stage of assembly and test. The thermal subsystem has been successfully tested, as well as the preliminary placement of the mirrors. Tests of the full SIR system are in progress.

In a representative laboratory setup tests have been conducted on SIR devices. Some example results, all of the same device and taken at 4.2 K, are given in the Figures below. Figure 8 shows the level of pumping by the FFO of the SIS and HM mixers as a function of FFO frequency. The required minimum pumping levels are shown as dashed lines. The plot shows that the FFO is able to sufficiently pump both the SIS and HM over almost the complete frequency range, though some optimization is still possible.

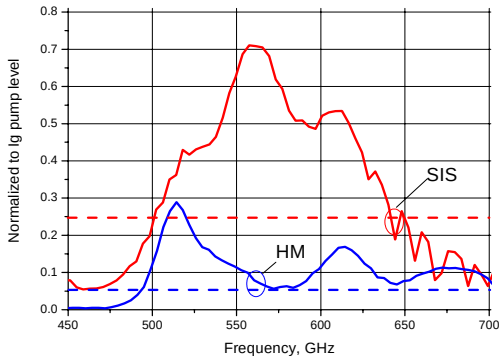

Figure 8: Level of pumping by the FFO of the SIS and HM mixers. The dashed lines indicate the minimum required levels.

Figures 9a and 9b show the FTS response and the noise performance of the SIS mixer, anti-correlated as expected. The structure on the plots indicate that improvements are still needed in the design of the antenna-mixer and matching circuits. Ongoing development of the SIR chips will concentrate on performance optimization of the three interdependent superconducting elements on one chip and the microstrip coupling circuitry between them.

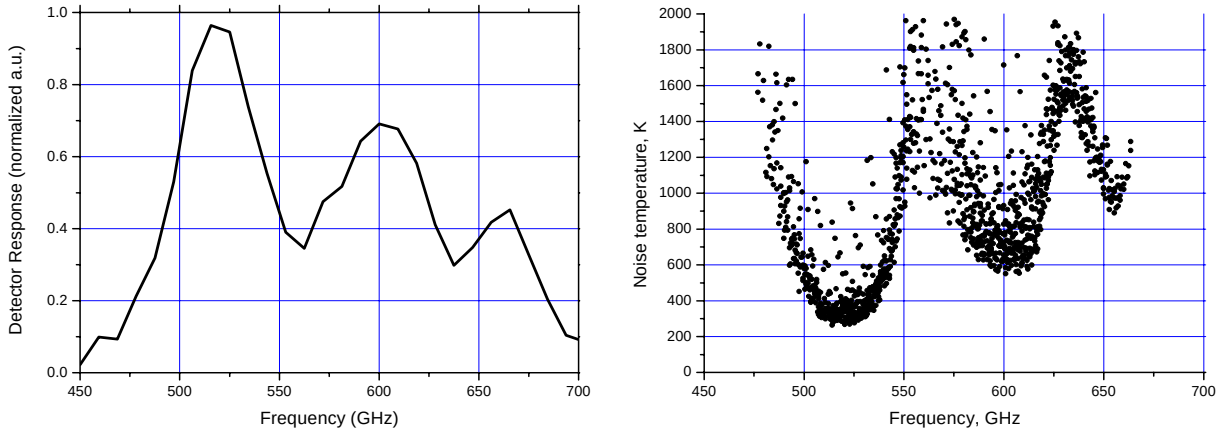

Figure 9a, left: FTS response of the SIS mixer. Figure 9b, right: Noise temperature of the SIR system, not including fore optics.

ACKNOWLEDGEMENTS

The authors acknowledge the contributions of all TELIS colleagues at the SRON, IREE, DLR and RAL laboratories, as well as those at IPM/RAS and Oleksandr Pylypenko of the Institute Iceberg, Kiev, Ukraine.

The work was supported in parts by the RFBR projects 03-02-16748; INTAS project 01-0367, ISTC projects # 2445, 3174 and the President Grant for the Scientific School 1344.2003.2.

REFERENCES

1. For info on SBUV see: http://code916.gsfc.nasa.gov/Public/Space_based/sbuv/sbuv.html; for info on TOMS see: http://toms.gsfc.nasa.gov/.
2. For info on ERS-2/GOME see: http://earth.esa.int/ers/eeo4.96/
3. For info on ENVISAT/Sciamachy see http://envisat.esa.int/instruments/sciamachy/ and http://www-iup.physik.uni-bremen.de/sciamachy/index.html
4. For info on EOS-Aura/OMI see: http://aura.gsfc.nasa.gov/instruments/omi/index.html
5. For info on MetOp/GOME-2 see: http://www.esa.int/esaME/gome-2.html
6. For info on ENVISAT/MIPAS see: http://envisat.esa.int/instruments/mipas/ and http://www-imk.fzk.de/asf/ame/

7. For info on EOS-Aura /TES see: http://aura.gsfc.nasa.gov/instruments/tes/index.html
8. For info on MetOp/IASI see: http://www.esa.int/esaME/iasi.html
9. For info on UARS/MLS, EOS-Aura /MLS and CAMEO/SMLS see: http://mls.jpl.nasa.gov/
10. U. Frisk et al., *The Odin satellite: Radiometer design and test*, Astronomy&Astrophysics A&A 402, L27-L34 (2003), at http://www.edpsciences.org/articles/aa/full/2003/18/aaODIN2/aaODIN2.html?access=ok
11. For info on JEM/SMILES see: http://smiles.tksc.nasda.go.jp/
12. For info on Herschel/HIFI see: http://www.sron.nl/divisions/lea/hifi/
13. J. R. Pardo, L. Pagani, G. Olofsson, P. Febvre, and J. Tauber, *"Balloonborne submillimeter observations of upper stratospheric O_2 and O_3"* , *J. Quant. Spectrosc. Radiat. Transf.*, vol. 67, pp. 169–180, 2000 and Deschamps A et al. *"A balloon experiment searching for the 425GHz O2 line with an SIS Receiver"*, proc. of the ESA Workshop on Millimeter Wave Technology and Applications, Espoo, Finland, May 1998.
14. For info on ASUR see: http://www.iup.physik.uni-bremen.de/asur/asurhome_e.html
15. For info on SMILES see: http://www2.nict.go.jp/dk/c214/bsmiles/
16. For info on MIPAS-B see http://www-imk.fzk.de/asf/mipas-b/mipas-b.htm
17. M.E. Summers, R.R. Conway, D.E. Siskind, M.H. Stevens, D. Offermann, M. Riese, P. Preusse, D.F. Strobel, J.M. Russell III, *"Implications of Satellite OH Observations for Middle Atmospheric H_2O and Ozone*", Science, Vol 277 (1997) 1967-1970.
18. G.P. Smith, M. Frenklach, R. Feeley, A. Packard, and P. Seiler, *"A System Analysis Approach for Atmospheric Observations and Models: the Mesospheric HOx Dilemma"*, submitted for publication in *Journal of Geophysical Research (Atmospheres)*, June 2005.
19. F.W. Irion, M.R. Gunson, C.P. Rinsland, Y.L. Yung, M.C. Abrams, A.Y. Chang, and A. Goldman, *"Heavy Ozone enrichments from ATMOS infrared solar spectra"*, Geophysical Research Letters, Vol 23 (1996), 2377 - 2380.
20. K. Mauersberger, B. Erbacher, D. Krankowsky, J. Günther, and R. Nickel, *"Ozone Isotope Enrichment: Isotopomer-Specific Rate Coefficients*". *Science* 283 (1999) 370-372.
21. P. Yagoubov, H. van de Stadt, R. Hoogeveen, V. Koshelets, M. Birk, and A. Murk, *"Optical design of sub-millimeter spectrometer for limb sounder"*, in 28th ESA Antenna Workshop on Space Antenna Systems and Technologies, Noordwijk (NL), May 2005.
22. P.A. Yagoubov, W.-J. Vreeling, H. van de Stadt, R.W.M. Hoogeveen, O.V. Koryukin, V. P. Koshelets, O.M. Pylypenko, A. Murk, *"550-650 GHz spectrometer development for TELIS"*, proceedings of the 16th Intern. Conf. on Space Terahertz Technology, Göteborg, Sweden, May 2-4, 2005.
23. A. Murk, P. Yagoubov, U. Mair, M. Birk, G. Wagner, H. van de Stadt, R. Hoogeveen, and N. Kämpfer, *"Antenna simulations for the THz and submm limb sounder TELIS"*, in 28th ESA Antenna Workshop on Space Antenna Systems and Technologies, Noordwijk (NL), May 2005.
24. B.N. Ellison, B.P. Moyna, D.N. Matheson, A. Jones, S.M.X. Claude, C. Mann, B.J. Kerridge, R. Siddans, R. Munro, and W.J. Reburn, "*Development of a high sensitivity airborne SIS receiver to detect ClO and BrO*", Proc. of 2nd ESA Workshop on Millimetre Wave Technology and Applications, Espoo, Finland, May 1998.
25. ESA report SP-1257 (4) *"ACECHEM – Atmospheric Composition Explorer for Chemistry and Climate Interaction"*, 2001, at http://www.estec.esa.nl/granada_2001/reports/screen/sp_1257_4_acechemsc.pdf
26. V.P. Koshelets, P.N. Dmitriev, A.B. Ermakov, L.V. Filippenko, O.V. Koryukin, A.V. Khudchenko, M.Yu. Torgashin, P.A. Yagoubov, R.W.M Hoogeveen, and W. Wild, "*Superconducting Submm Integrated Receiver with Phase-Locked Flux-Flow Oscillator for TELIS*", proceedings of the 16th Intern. Conf. on Space Terahertz Technology, Göteborg, Sweden, May 2005, and http://www.cplire.ru/html/lab234 /publications.htm
27. H. Richter, A. Semenov, H.-W. Hübers, K.V. Smirnov, G.N. Goltsman, B.M. Voronov, *"Phonon Cooled Hot-Electron Bolometric Mixer for 1-5 THz"*, 2004 Joint 29th Int. Conf. on Infrared and Millimeter Waves and 12th Int. Conf. on Terahertz Electronics, pages 241-244.
28. See http://www.omnisys.se/
29. See http://www.ticra.com/
30. M. J. M. van der Vorst. *"Integrated Lens Antennas for Submillimeter- wave Applications"*, PhD thesis, Elect. Eng. Dept., Eindhoven Univ. Technol., Eindhoven, The Netherlands, 1999.
31. V.P. Koshelets, S.V. Shitov, A.V. Shchukin, L.V. Filippenko, P.N. Dmitriev, V.L. Vaks, J. Mygind,

A.B. Baryshev, W. Luinge, H. Golstein, "*Flux Flow Oscillators for Sub-mm Wave Integrated Receivers*", *IEEE Trans. on Appl. Supercond.* **9**, 4133–4136 (1999).

32. L.S. Rothman, D. Jacquemart, A. Barbe, D. Chris Benner, M. Birk, L.R. Brown, M.R. Carleer, C. Chackerian, K. Chance, V. Dana, V.M. Devi, J.-M. Flaud, R.R. Gamache, A. Goldman, J.-M. Hartmann, K.W. Jucks, A.G. Maki, J.-Y. Mandin, S.T. Massie, J. Orphal, A. Perrin, C.P. Rinsland, M.A. H. Smith, J. Tennyson, R.N. Tolchenov, R.A. Toth, J. Vander Auwera, P. Varanasi, G. Wagner, "*The HITRAN 2004 Molecular Spectroscopic Database*", Journal of Quantitative Spectroscopy and Radiative Transfer, in press (2005).